Synthesis, Separation and Characterization of Small and Highly Fluorescent Nitrogen-Doped Carbon Quantum Dots

Francesca Arcudi,* Luka Đorđević and Maurizio Prato*[a]

Dedicated to Prof. Giacinto Scoles on the occasion of his 80th birthday

Abstract: A facile bottom-up approach to carbon quantum dots (CQDs) is reported, using a microwave-assisted protocol under controlled conditions. The as-prepared nitrogen-doped CQDs (NCQDs) show narrow size-distribution, abundant surface traps and functional groups, resulting in tunable fluorescent emission and excellent solubility in water. Moreover, we present a general method for the separation of NCQDs by low-pressure size-exclusion chromatography, leading to an even narrower size distribution, different surface composition and optical properties. They display among the smallest size and the highest FLQYs reported so far. ^{13}C-enriched starting materials produced N[13]CQDs suitable for thorough NMR studies, which gave useful information on their molecular structure. This work provides a new avenue to size and surface controllable and structurally defined NCQDs for applications in areas such as optoelectronics, biomedicine and bioimaging.

Extensive effort has been devoted to obtain non-toxic fluorescent nanomaterials, as an alternative to the popular semiconductor-based quantum dots (QDs). Carbon quantum dots (CQDs) are recently discovered nanocarbons that comprise discrete, quasispherical nanoparticles with size below 10 nm.[1] CQDs were first discovered during the purification of single-walled carbon nanotubes through preparative electrophoresis in 2004[2] and, due to their interesting properties, have gradually become a prominent new member of the nanocarbon family.[3–5]

Compared to traditional semiconductor QDs and organic dyes, photoluminescent CQDs are potentially superior in terms of biological properties, high (aqueous) solubility, robust chemical inertness, facile modification and high resistance to photobleaching.[4,6–8] Their unique properties give them a high potential in biomedicine, optronics and catalysis.[9–17] A very interesting property of CQDs is their tunable emission, characterized by multi fluorescence (FL) colors under varied excitation wavelength.

A number of different synthetic protocols have been developed and reported for the preparation of CQDs, usually classified as "top-down" or "bottom-up".[4,16] However, the structure and size of CQDs are still difficult to control. Therefore, a simple and cost-effective process, giving high quality and homogeneous nanodots remains a challenge.

To improve the fluorescence efficiency of CQDs two approaches are usually employed and involve surface modification and/or element doping.[1,18,19] Nitrogen doping has been reported to give excellent optical properties and usually blue shifted fluorescence, though most of the times nitrogen atoms are introduced under harsh conditions.[20–23] Amino acids are ideal carbon and nitrogen sources for CQDs due to their low cost and abundance.[23,24] Moreover, molecules containing primary amines allow simultaneous nitrogen doping and surface passivation during the synthetic process.[25]

The use of microwaves (MW) is a possible alternative synthetic approach, which would avoid multi-step synthesis and would benefit of features such as faster rates, milder conditions and low energy consumption.[25–28]

Herein, we report a simple bottom-up method for highly fluorescent nitrogen-doped CQDs (NCQDs), using a MW reactor under controlled conditions, without the need of sophisticated equipment and/or additional surface passivation. We also report the separation of NCQDs with low-pressure gel permeation chromatography, which results in an effective strategy for quasi-monodispersed NCQDs with improved optical properties. Finally, NMR experiments carried out on ^{13}C-enriched NCQDs allowed us to obtain important structural information.

Arginine (Arg) and ethylenediamine (EDA) were used as carbon and nitrogen sources. The heterogeneous solution underwent thermal carbonization of the precursors and led to nucleation. Finally, the nuclei grew by diffusion of other molecules towards the surface of the nanoparticles. In the process of microwave heating, the solution changed color from transparent to dark brown as a result of the formation of NCQDs (Figure S1). The MW parameters were optimized to obtain the desired properties of the final material, in terms of optical performance (vide infra). Appropriate viscosity and temperature control are needed for a uniform carbonization process that leads to the formation of NCQDs itself. Fluorescent NCQDs were obtained at 240 °C, 26 bar, 200 W with a MW heating time of 180 seconds using water as reaction medium (see Supplementary Information for experimental details). Large carbon nanoparticles were removed by filtration and the yellow solution was dialyzed against Milli-Q water. The obtained NCQDs exhibited a high solubility in water (up to 80 mg/mL) and also in common polar organic solvents.

In order to gain unprecedented structural information, we prepared ^{13}C-enriched NCQDs (N[13]CQDs) for ^{13}C-NMR investigations (Figure 1), starting with fully ^{13}C-enriched Arg and EDA. A tentative interpretation of a representative structural unit of NCQDs is reported in Figure 2, with a very general peak assignment. Typically, ^{13}C-NMR spectra of N[13]CQDs consist of an aliphatic region (Figure 2, C_a), with carbon atoms connected to heteroatoms (Figure 2, C_b) or to an aromatic core (Figure 2, C_c) and an aromatic region (Figure 2, C_{e-h}). First of all, the

[a]   Ms. F. Arcudi, Mr. L. Đorđević and Prof. M. Prato
        Department of Chemical and Pharmaceutical Sciences, INSTM UdR
        Trieste, University of Trieste
        Trieste 34127 (Italy)
        E-mail: francesca.arcudi@phd.units.it, prato@units.it

        Prof. M. Prato
        Carbon Nanobiotechnology Laboratory, CIC biomaGUNE, Paseo de
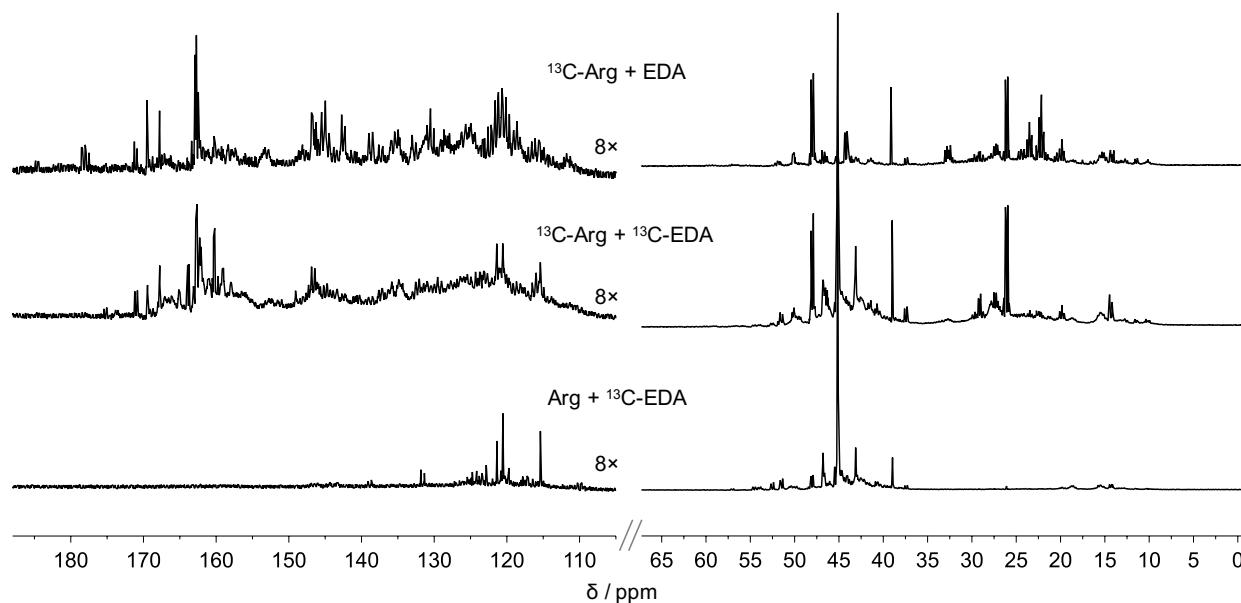   Miramón 182, 20009 Donostia-San Sebastian (Spain)

Figure 1. ^{13}C-NMR spectra of N^{13}CQDs prepared starting from ^{13}C-Arg and EDA (top), ^{13}C-Arg and ^{13}C-EDA (middle) and Arg and ^{13}C-EDA (bottom). The intensity of the aromatic region was increased 8 times in order to facilitate the visualization.

contribution of each component was evaluated, using separated and combined ^{13}C-Arg and ^{13}C-EDA (Figure 1, and Figures S3-S6). Figure 1-top shows the ^{13}C-NMR spectrum of NCQDs produced using only ^{13}C-enriched Arg. It is clear that the aromatic core and the aliphatic as well as the carbonyl regions mainly originate from Arg. While EDA (Figure 1-bottom) mostly contributes to the typical region of aliphatic carbon atoms connected to heteroatoms, signals arising from EDA were also found in the aromatic core of N^{13}CQDs. Additional bidimensional experiments (^{1}H-^{13}C) revealed numerous H-C correlations both by direct (HSQC, Figure 2, H_a-C_a H_b-C_b H_c-C_c, Figures S7-S9) or through multiple-bond correlations (HMBC, Figure 2, H_a-C_b-C_c H_c-C_d-C_e, Figures S10-S12). Remarkably, protons that lie in the aliphatic region and close to heteroatoms were found to correlate with the aromatic sp^2-carbon core (Figure 2, red lines). Analogous data was obtained from ^{13}C-^{13}C one bond correlation (INADEQUATE, Figure 2, C_a-C_c C_c-C_d C_f-C_g-C_h Figures S13-S15). Additionally, Diffusion-Ordered Spectroscopy (DOSY, Figure S16) was performed through ^{1}H-^{13}C multiple-bond correlation in order to unambiguously assign the signals to macromolecular species. As a provisional conclusion, we can say that our NCQDs are polymeric, rounded-shaped materials, containing both aliphatic and aromatic regions with many amino groups amenable to further functionalization.

Atomic force microscopy (AFM) confirmed the round shape and showed that NCQDs (as-prepared NCQDs, from now on ap-NCQDs) have a rather homogeneous size distribution (Figure 2a,e,i). By statistical analysis of the height of about one hundred nanoparticles, we determined an average size of 2.47 ± 0.84 (FWHM: 1.977).

The crude mixture of NCQDs produced after MW treatment was also separated by means of low pressure gel filtration chromatography using a column packed with Sephadex LH-20 and operating at a pressure of 150 psi. According to their elution time we collected three fractions, named NCQDs**1**, NCQDs**2** and NCQDs**3**, whose size was analyzed by AFM. AFM images, height profiles and size distributions of the three fractions are reported in Figure 2b-d,f-h,j-l. Average sizes of 2.65 ± 0.48

(FWHM: 1.141), 2.04 ± 0.57 (FWHM: 1.345), 1.24 ± 0.43 (FWHM: 1.013) were determined for NCQDs**1**, NCQDs**2** and NCQDs**3**, respectively. These are among the smallest CQDs ever reported.[5,29]

The structure and composition of the ap-NCQDs, as well as the separated NCQDs**1-3,** were determined by FT-IR spectroscopy and X-ray photoelectron spectroscopy (XPS). FT-IR spectra (Figure 3a) show that ap-NCQDs have many oxygenated functional groups on their surface such as carboxylic acid, epoxy, alkoxy, hydroxyl and carbonyl groups. Absorptions at 1194 and 1111 cm^{-1} can be attributed to C-O-C bond, while absorptions at 1350 and 1318 cm^{-1} confirm the presence of C-O bonds. Moreover, the absorption peaks at 1655, 1704 and 1767 cm^{-1} are indicative of C=O bonds, whereas the broad peak centered at 3299 cm^{-1} revealed O-H/N-H bonding. In addition, C-N (1492 and 1437 cm^{-1}) and C=N (1557 cm^{-1}) functional groups can be identified, while peaks at 2932 and 2862 cm^{-1} are related to the C–H bond stretching vibrations.

The separated NCQDs**1**, NCQDs**2** and NCQDs**3** have similar IR spectra, suggesting a similar functional group distribution (Figure S17). To further confirm the functional groups present on the surface of NCQDs, XPS characterization was carried out. From the full-scan XPS spectra of ap-NCQDs (Figure 3b) C, N, O are detected with peaks at 286.8 eV (C1s), 400.33 eV (N1s), and 532.34 eV (O1s) respectively. To determine the C and N configurations in the ap-NCQDs, C1s and N1s spectra were analyzed (Figure 3c-d). The XPS spectrum of C1s can be deconvoluted into five surface components corresponding to sp^2(C=C) at 284.5 eV, sp^3 (C-C, and C-H) at 285.5 eV, C-O/C-N at 286.2 eV, C=O/C=N at 288.3 eV, as well as COOH at 290.5 eV. The N1s spectrum can be deconvoluted into four peaks centered at 398.3, 399.6, 400.5, 401.9 eV corresponding to C=N, NH$_2$, C-N-C and N-C$_3$ respectively.[21,22,30] The surface components of ap-NCQDs, as determined by XPS, are in good agreement with the FT-IR and NMR results. The presence of primary amino groups was confirmed by a positive Kaiser test. From this highly sensitive colorimetric test, it was possible to estimate a value of 1350 μmol/g of amino groups: their presence
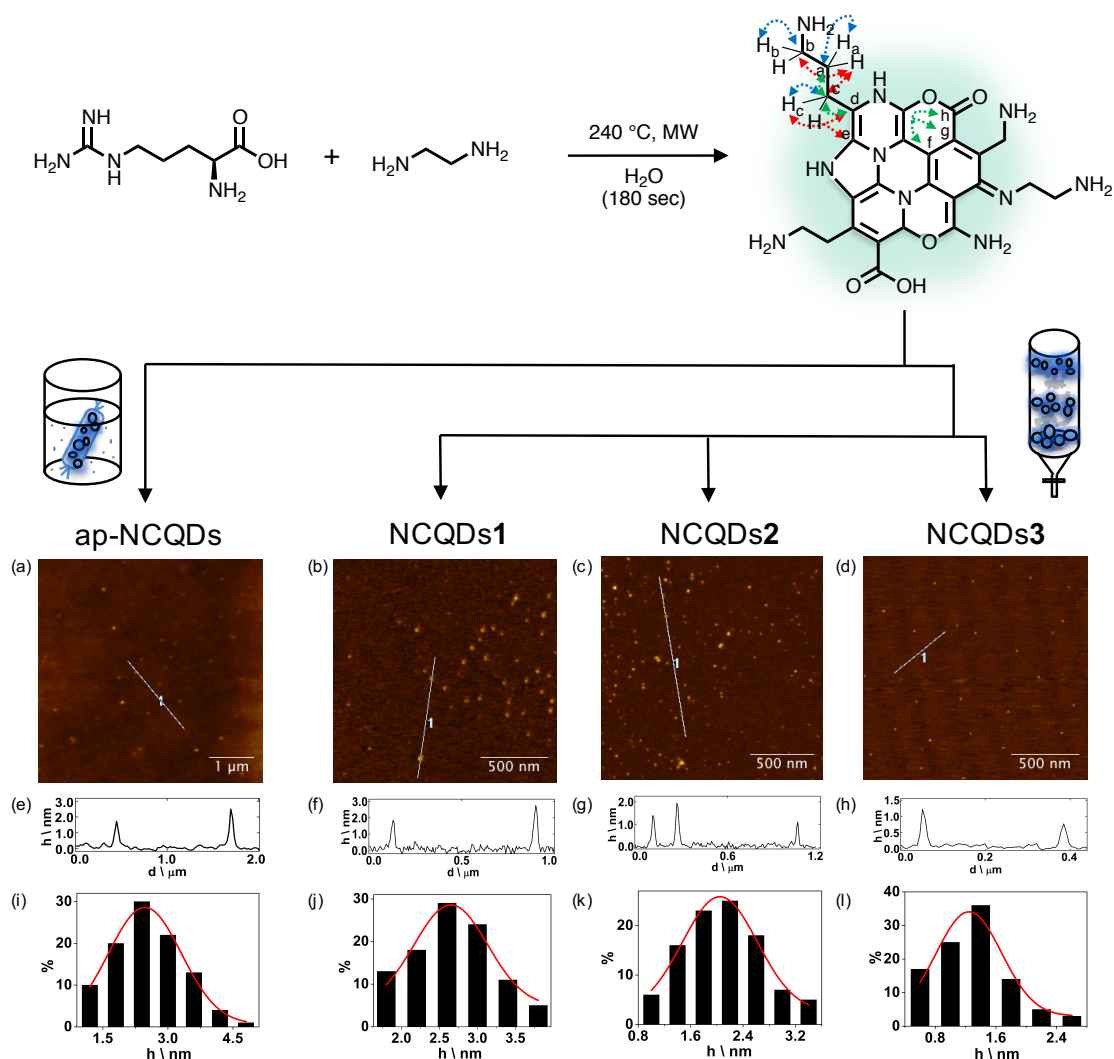
Figure 2. Reaction scheme for NCQDs and their functional groups representation. Representative structural correlations found in NMR experiments are reported in dashed arrows (HSQC blue lines, HMBC red lines and INADEQUATE green lines). a-d) Tapping mode AFM images of ap-NCQDs (5.0 x 5.0 μm) and NCQDs**1-3** (1.7 x 1.7 μm) on a mica substrate; e-h) Height profiles of ap-NCQDs and NCQDs**1-3**; i-l) Size histograms of ap-NCQDs and NCQDs**1-3** with curves fit to the data using a Gaussian model.

makes NCQDs prompt to the easy insertion of further functional groups and/or interesting molecules/ions through standard organic chemistry protocols.[28] The cyclic voltammogram of ap-NCQDs shows two irreversible peaks corresponding to the oxidation (+1.14 V vs SCE) and reduction (-2.52 V vs SCE) of amines (Figure S18). The high current in oxidation and the steep slope of the peak are remarkable, demonstrating the easy way to oxidize a high quantity of amino groups on the surface.

The XPS survey spectra for NCQDs**1**, NCQDs**2** and NCQDs**3** and spectra of C1s and N1s are reported in Figure S19,20, while the XPS data for NCQDs**1-3**, along with that of ap-NCQDs are collected in Table 1. The results show that all the NCQDs contain similar multiple oxygen and nitrogen functional groups on particle surface but with different contents, a result which is consistent with the FT-IR measurements.

The functional groups located at the surface of NCQDs act as a "passivation" layer, which improves their hydrophilicity and stability in aqueous systems as well as their efficient photoluminescence properties.[6]

The aqueous solutions (0.5 mg/mL) of ap-NCQDs appeared yellow in daylight and remained stable for several weeks, with no change in their spectral features. Upon excitation under a 365 nm UV lamp, ap-NCQDs emit with strong blue luminescence, while the UV-Vis spectrum of ap-NCQDs show an absorption band at 286 nm, ascribed to the $\pi-\pi^*$ transition of the conjugated C=C units from the carbon core (Figure 4a).[1,5]

Fluorescence (FL) is one of the most fascinating features of CQDs and the excitation wavelength dependence of the emission and intensity is a common phenomenon observed in CQDs.[6,31] CQDs produce multi-fluorescence colors under different excitation wavelengths and this behavior may arise not only from particles of different size but also from a distribution of different emissive domains on each carbon dots. This property implies that the emission of CQDs can be tuned by changing the excitation wavelength since the emission arises from different surface emissive traps.

The luminescence properties of the ap-NCQDs have been explored. A broad emission peak at 356 nm is observed when the sample is excited at the optimal excitation wavelength (300 nm, Figure 4b). The fluorescence peaks shift from 356 nm to 474 nm when the excitation wavelength changes from 300 to 420 nm and the fluorescence intensity decreased as the peak
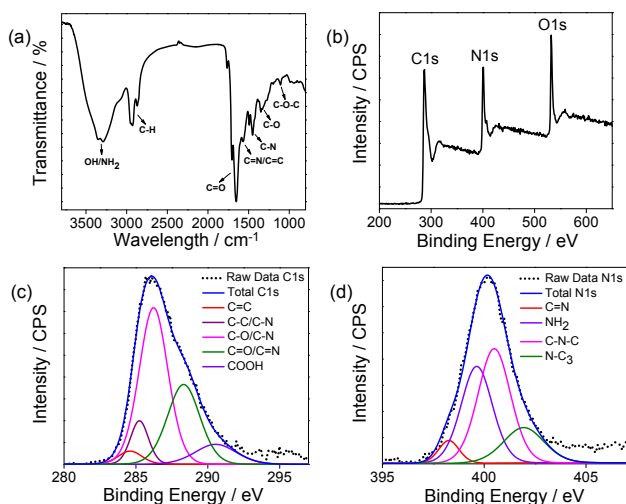
Figure 3. a) FTIR spectra of ap-NCQDs; b) XPS survay of ap-NCQDs; c) deconvoluted C1s spectra of ap-NCQDs; d) deconvoluted N1s spectra of ap-NCQDs.

red shifts. The many kinds of functional groups presented on the surface of ap-NCQDs have different surface states energy levels, which results in a series of emissive traps that dominate the emission at different excitation wavelengths and explain the excitation wavelength dependent phenomenon of ap-NCQDs. The fluorescence quantum yield (FLQY) was found to be 0.17, using a reported procedure and quinine sulphate as the reference (see Supporting Information).[32,33]

As expected, size and functional groups affect the optical properties. Figure 4c shows NCQDs**1-3** UV-Vis absorption spectra. NCQDs**1** have an absorption peak located at 315 nm, while NCQDs**2** have two peaks at 285 and 315 nm and NCQDs**3** have three peaks at 253, 278, and 328 nm. These peaks are most probably related to the electron transitions from π (or n) to π^* of C=C and C=O.[1,5]

Table 1. Percentage of C, N, O atoms in ap-NCQDs and NCQD**1-3**, as determined by XPS measurements.

	ap-NCQDs	NCQDs1	NCQDs2	NCQDs3
C%	68.0	65.9	68.7	63.9
C=C	3.4	21.7	4.1	15.8
C-C	8.7	25.1	25.6	6.4
C-O C-N	50.1	28.2	53.0	56.2
C=O C=N	28.7	24.9	14.7	21.6
COOH	9.1		2.5	
N%	16.1	11.1	9.0	7.0
C=N	5.4		10.6	
NH₂	35.0	40.6	20.4	17.8
C-N-C	43.1	46.7	57.1	70.7
N-C3	16.5	12.7	11.9	11.4
O%	15.9	23.0	22.3	29.0

Tipically, as the particles become smaller, the luminescence energies are blue shifted to higher energies.[34] However, the FL mechanism of CQDs is affected also by zigzag edge sites and defects effect. Hence, size-indipendent FL could be also
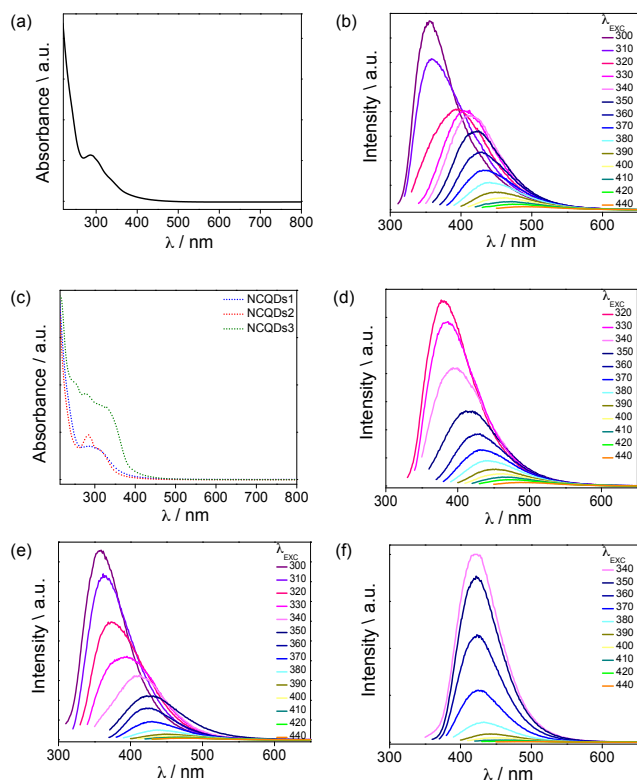

Figure 4. a) UV-Vis absorption spectra of ap-NCQDs in water; b) FL spectra of ap-NCQDs in water (298 K) at different excitation wavelengths; c) UV-Vis absorption spectra of NCQDs**1-3** in water; d-f) FL spectra of NCQDs**1-3** in water (298 K) at different excitation wavelengths.

observed because the surface state emission can play a predominant role in the FL properties.[35]

NCQDs**1-2** show a clear excitation-dependent emission spectra, whereas NCQDs**3** exhibit an almost excitation-independent behavior. Each sample has its optimal emission for a characteristic excitation wavelength, revealing the presence of different energy levels corresponding to the maximum transition probability (Figure 4d-f). The surface of NCQDs significantly affects the FL properties since it determines the trapping of excitons under excitation. Therefore, the radiative recombination of those surface-trapped excitons leads to FL with the corresponding energy. NCQDs**1**, NCQDs**2** and NCQDs**3** exhibited their most intense emission at 380 nm (excitation at 320 nm), 357 nm (excitation at 300 nm), 421 nm (excitation at 340 nm), respectively. The FLQYs of NCQDs**1**, NCQDs**2** and NCQDs**3** were 0.07, 0.31 and 0.46. To the best of our knowledge, the latter is among the highest FLQY values so far reported for CQDs.[4] Figure 5 clearly shows the increased emitted blue luminescence from NCQDs**1** to NCQDs**3** upon excitation under a 365 nm UV lamp.

As reported in Table 1, NCQDs**1-3** have similar functional groups and nitrogen content. The QYs increase with the reduced amount of amine groups, with NCQDs**3** having the highest degree of surface oxidation, resulting in more surface defects, which can trap more excitons leading to higher FL quantum yield.[36]

In summary, we have described a straightforward, simple and controllable method to prepare NCQDs under microwave irradiation. Using this approach, NCQDs could be obtained within three minutes without the need of sophisticated equipment or additional surface passivation. In addition, we

have reported a general method for the separation of three fractions of NCQDs with different size and properties by low-pressure gel permeation chromatography. These NCQDs are narrowly size-distributed and their abundant surface traps and functional groups endowed them with tunable fluorescent emission, bright luminescence with quantum yield as high as 0.46 and excellent solubility in water and in common polar organic solvents. We have demonstrated that the fluorescence strongly depends on the surface states of the NCQDs since their optical properties are affected by the competition among different emission centers and traps. This work provides a new route to size and surface controllable NCQDs. Their superior optical properties, coupled with their low cost and ease of labeling, should enable their use in numerous applications, which are currently underway in our laboratory.
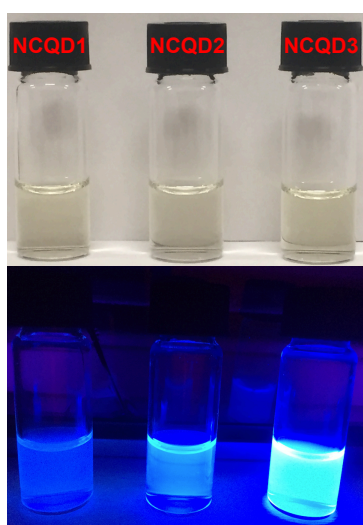

Figure 5. Photographs of NCQDs**1**, NCQDs**2**, NCQDs**3** in daylight (upper part) and under UV light (365 nm) illumination (bottom part).

Acknowledgements

[1]   Y.-P. Sun, B. Zhou, Y. Lin, W. Wang, K. A. S. Fernando, P. Pathak, M. J. Meziani, B. A. Harruff, X. Wang, H. Wang, et al., *J. Am. Chem. Soc.* **2006**, *128*, 7756–7757.

[2]   X. Xu, R. Ray, Y. Gu, H.J. Ploehn, L. Gearheart, K. Raker, W. A. Scrivens, *J. Am. Chem. Soc.* **2004**, *126*, 12736–12737.

[3]   V. Georgakilas, J. a. Perman, J. Tucek, R. Zboril, *Chem. Rev.* **2015**, *115*, 4744–4822.

[4]   S. Y. Lim, W. Shen, Z. Gao, *Chem. Soc. Rev.* **2015**, *44*, 362–381.

[5]   P. Roy, P.-C. Chen, A. P. Periasamy, Y.-N. Chen, H.-T. Chang, *Mater. Today* **2015**, *18*, 447–458.

[6]   S. N. Baker, G. A. Baker, *Angew. Chemie Int. Ed.* **2010**, *49*, 6726–6744; *Angew. Chemie* **2010**, *122*, 6876–6896.

[7]   S.-T. Yang, L. Cao, P. G. Luo, F. Lu, X. Wang, H. Wang, M. J. Meziani, Y. Liu, G. Qi, Y.-P. Sun, *J. Am. Chem. Soc.* **2009**, *131*, 11308–11309.

[8]   L. Cao, X. Wang, M. J. Meziani, F. Lu, H. Wang, P. G. Luo, Y. Lin, B. a Harruff, L. M. Veca, D. Murray, et al., *J. Am. Chem. Soc.* **2007**, *129*, 11318–11319.

[9]   J. Tang, B. Kong, H. Wu, M. Xu, Y. Wang, Y. Wang, D. Zhao, G. Zheng, *Adv. Mater.* **2013**, *25*, 6569–6574.

[10]   M. Zheng, S. Liu, J. Li, D. Qu, H. Zhao, X. Guan, X. Hu, Z. Xie, X. Jing, Z. Sun, *Adv. Mater.* **2014**, *26*, 3554–3560.

[11]   J. Lei, L. Yang, D. Lu, X. Yan, C. Cheng, Y. Liu, L. Wang, J. Zhang, *Adv. Opt. Mater.* **2015**, *3*, 57–63.

[12]   H. Li, X. He, Z. Kang, H. Huang, Y. Liu, J. Liu, S. Lian, C. H. A. Tsang, X. Yang, S.-T. Lee, *Angew. Chemie Int. Ed.* **2010**, *49*, 4430–4434; *Angew. Chemie* **2010**, *122*, 4532–4536.

[13]   F. Wang, Y. Chen, C. Liu, D. Ma, *Chem. Commun.* **2011**, *47*, 3502–3504.

[14]   X. Zhang, Y. Zhang, Y. Wang, S. Kalytchuk, S. V Kershaw, Y. Wang, P. Wang, T. Zhang, Y. Zhao, H. Zhang, et al., *ACS Nano* **2013**, *7*, 11234–11241.

[15]   X. Yu, J. Liu, Y. Yu, S. Zuo, B. Li, *Carbon N. Y.* **2014**, *68*, 718–724.

[16]   A. Zhao, Z. Chen, C. Zhao, N. Gao, J. Ren, X. Qu, *Carbon N. Y.* **2015**, *85*, 309–327.

[17]   P. G. Luo, F. Yang, S.-T. Yang, S. K. Sonkar, L. Yang, J. J. Broglie, Y. Liu, Y.-P. Sun, *RSC Adv.* **2014**, *4*, 10791.

[18]   H. Zheng, Q. Wang, Y. Long, H. Zhang, X. Huang, R. Zhu, *Chem. Commun.* **2011**, *47*, 10650–10652.

[19]   Y. Dong, H. Pang, H. Bin Yang, C. Guo, J. Shao, Y. Chi, C. M. Li, T. Yu, *Angew. Chem. Int. Ed. Engl.* **2013**, *52*, 7800–7804; *Angew. Chemie* **2013**, *125*, 7954–7958.

[20]   X. Chen, Q. Jin, L. Wu, C. Tung, X. Tang, *Angew. Chem. Int. Ed. Engl.* **2014**, *53*, 12542–12547; *Angew. Chemie* **2014**, *126*, 12750–12755.

[21]   G. S. Kumar, R. Roy, D. Sen, U. K. Ghorai, R. Thapa, N. Mazumder, S. Saha, K. K. Chattopadhyay, *Nanoscale* **2014**, *6*, 3384–3391.

[22]   J. Moon, J. An, U. Sim, S.-P. Cho, J. H. Kang, C. Chung, J.-H. Seo, J. Lee, K. T. Nam, B. H. Hong, *Adv. Mater.* **2014**, *26*, 3501–3505.

[23]   Y. Xu, M. Wu, Y. Liu, X.-Z. Feng, X.-B. Yin, X.-W. He, Y.-K. Zhang, *Chem. - A Eur. J.* **2013**, *19*, 2276–2283.

[24]   J. Jiang, Y. He, S. Li, H. Cui, *Chem. Commun.* **2012**, *48*, 9634–9636.

[25]   X. Zhai, P. Zhang, C. Liu, T. Bai, W. Li, L. Dai, W. Liu, *Chem. Commun.* **2012**, *48*, 7955–7957.

[26]   H. Zhu, X. Wang, Y. Li, Z. Wang, F. Yang, X. Yang, *Chem. Commun.* **2009**, 5118–5120.

[27]   S. Chandra, P. Das, S. Bag, D. Laha, P. Pramanik, *Nanoscale* **2011**, *3*, 1533–1540.

[28]   D. Mazzier, M. Favaro, S. Agnoli, S. Silvestrini, G. Granozzi, M. Maggini, A. Moretto, *Chem. Commun.* **2014**, *50*, 6592–6595.

[29]   Z. Yang, Z. Li, M. Xu, Z. Zhang, J. Zhang, Y. Su, F. Gao, H. Wei, L. Zhang, *Nano-Micro Lett.* **2013**, *5*, 247–259.

[30]   Y. Yang, J. Cui, M. Zheng, C. Hu, S. Tan, Y. Xiao, Q. Yang, Y. Liu, *Chem. Commun.* **2012**, *48*, 380–382.

[31]   V. Strauss, J. T. Margraf, C. Dolle, B. Butz, T. J. Nacken, J. Walter, W. Bauer, W. Peukert, E. Spiecker, T. Clark, et al., *J. Am. Chem. Soc.* **2014**, *136*, 17308–17316.

[32]   J. R. Lakowicz, *Principles of Fluorescence Spectroscopy Third Edition*, **2006**.

[33]   C. Würth, M. Grabolle, J. Pauli, M. Spieles, U. Resch-Genger, *Nat. Protoc.* **2013**, *8*, 1535–1550.

[34]   R. Ye, C. Xiang, J. Lin, Z. Peng, K. Huang, Z. Yan, N. P. Cook, E. L. G. Samuel, C.-C. Hwang, G. Ruan, et al., *Nat. Commun.* **2013**, *4*, 2943.

[35]   L. Tang, R. Ji, X. Li, G. Bai, C. P. Liu, J. Hao, J. Lin, H. Jiang, K. S. Teng, Z. Yang, et al., *ACS Nano* **2014**, *8*, 6312–6320.

[36]   S. Zhu, J. Zhang, X. Liu, B. Li, X. Wang, S. Tang, Q. Meng, Y. Li, C. Shi, R. Hu, et al., *RSC Adv.* **2012**, *2*, 2717–2720.